Decadal Variability in the Northeast Pacific in a Physical-Ecosystem Model: The Role of Mixed Layer Depth and Trophic Interactions

Michael Alexander[a], Antonietta Capotondi[a], Arthur Miller[b], Fei Chai[c], Richard Brodeur[d], and Clara Deser[e]

a NOAA, Earth System Research Laboratory, Boulder, CO 80305, USA

b Scripps Institution of Oceanography, University of California, San Diego, La Jolla, CA 92093, USA

c School of Marine Sciences, University of Maine, Orono, ME 04469, USA

d NOAA, Northwest Fisheries Science Center, Hatfield Marine Science Center, Newport, OR 97365, USA

e NCAR/Climate and Global Dynamics Division, Boulder, CO 80307, USA

Submitted to the Journal Geophysical Research – Oceans

May 2007

Corresponding Author:
Michael Alexander
NOAA, Earth System Research Laboratory
Physical Science Division
R/PSD1
325 Broadway
Boulder, CO 80305-3328
USA
Michael.Alexander@noaa.gov

3

Abstract

A basin-wide interdecadal change in both the physical state and the ecology of the North Pacific occurred near the end of 1976. Here we use a physical-ecosystem model to examine whether changes in the physical environment associated with the 1976-77 transition influenced the lower trophic levels of the food web and if so by what means. The physical component is an ocean general circulation model, while the biological component contains ten compartments: two phytoplankton, two zooplankton, two detritus pools, nitrate, ammonium, silicate and TCO_2. The model is forced with observed atmospheric fields during 1960-1999. During spring, there is a ~40% reduction in plankton biomass in all four plankton groups in spring during 1977-88 relative to 1970-76 in the central Gulf of Alaska (GOA). The epoch difference in plankton appears to be controlled by the mixed layer depth. Enhanced Ekman pumping after 1976 caused the halocline to shoal, and thus the mixed layer depth did not penetrate as deep in the central GOA during late winter. As a result, more phytoplankton remained in the euphotic zone and phytoplankton biomass began to increase earlier in the year after the 1976 transition. Zooplankton biomass also increased but then grazing pressure led to a strong decrease in phytoplankton by April followed by a drop in zooplankton by May: essentially the mean seasonal cycle of plankton biomass was shifted earlier in the year. Finally, plankton concentrations rebounded slightly after 1976, leading to a small increase in zooplankton biomass during summer in 1977-88 relative to 1970-76.

1. Introduction

Studies conducted over the past 15-20 years have provided a growing body of evidence for decadal climate variability across the Pacific Basin [e.g. *Trenberth*, 1990, *Graham*, 1994, *Zhang et al.*, 1997; *Deser et al.*, 2004]. The most prominent mode of decadal variability in the North Pacific was termed the Pacific Decadal Oscillation (PDO) by *Mantua et al.* [1997] based on transitions between relatively stable states of the leading pattern of sea surface temperature (SST) anomalies. The 1976-77 transition or "regime shift" was especially pronounced, with an increase in the strength of the atmospheric circulation over the North Pacific that resulted in basin-wide changes in ocean temperatures, currents and mixed layer depth [e.g. *Miller et al.*, 1994; *Trenberth and Hurrell*, 1994; *Polovina et al.*, 1995; *Deser et al.*, 1996, 1999]. These climatic changes had a pervasive effect on marine ecosystems from phytoplankton to the top trophic levels [e.g. *Mantua et al.*, 1997; *Hare and Mantua*, 2000; *Benson and Trites*, 2002].

While the dynamics underlying Pacific decadal variability have not been fully resolved, changes in the physical state of the ocean clearly influence the primary and secondary production in the North Pacific. For example, total chlorophyll a, a proxy for phytoplankton biomass, nearly doubled in the central North Pacific from 1968 to 1985 [*Venrick et. al.*, 1987]. *Brodeur and Ware* (1992), *Brodeur et al.* [1996] and *Rand and Hinch* [1998] found that the zooplankton biomass in summer was relatively high in the central portion of the Gulf of Alaska (GOA) during 1956-1962, while in 1980-1989 the biomass was greatest along the edges of the Alaskan Gyre. Overall, the zooplankton biomass nearly doubled over the northeast Pacific in the 1980s relative to the late 1950s

and early 1960s. *McFarlane and Beamish* [1992] also found that the copepod biomass increased after the winter of 1976-77 in the Gulf of Alaska. In contrast, *Sugimoto and Tadokoro* [1997], found a decrease in both phytoplankton and zooplankton biomass in the northeast Pacific during the summers of 1980-1994 relative to those in 1960-1975. Some of the differences between these estimates of decadal variations may be due to the large interannual and spatial variability of zooplankton biomass, especially given the limited number of measurements.

Several physical/chemical factors may influence primary productivity in the Pacific on interannual to decadal time scales, including temperature, sunlight, macronutrients such as nitrogen and silica, and micronutrients, especially iron [see reviews by *Francis et al.*, 1998; *Miller et al.*, 2004]. Vertical mixing, and the mixed layer depth (MLD) in particular, are critical in linking the physical/chemical and biological processes [e.g. *Mann*, 1993; *Steele and Henderson*, 1993; *Gargett*, 1997]. If the mixed layer is too deep, phytoplankton will be transported beneath the euphotic zone inhibiting their growth due to the absence of light, but if it is too shallow, not enough nutrients will be mixed into the surface layer from below to sustain photosynthesis. In addition, if the MLD is sufficiently shallow in late winter for photosynthesis to occur and the resulting phytoplankton biomass is adequate to sustain zooplankton populations, then when the mixed layer shoals in spring, grazing by zooplankton can limit algal growth rates [e.g. *Parslow*, 1985; *Frost*, 1991; *Fasham*, 1995].

Several studies have emphasized the impact of changes in MLD during 1976-77 on the lower trophic levels of the North Pacific ecosystems [*Venrick et al.*, 1987; *Polovina et al.*, 1994]. *Brodeur and Ware* [1992] hypothesized that changes in wintertime MLD over

the northeast Pacific could impact the micronutrient supply and/or change the rate of primary productivity and the efficiency of zooplankton grazing in spring. *Polovina et al.* [*1*995] indicated that shoaling of the mixed layer in winter post 1976-77 could significantly enhance productivity in the Gulf of Alaska by increasing the light available for photosynthesis based on MLD estimated from temperature profiles and a plankton population dynamics model. However, the MLD is influenced by salinity in subarctic waters and it is unclear whether there is sufficient variability in the late winter MLD in the northeast Pacific to significantly impact primary and secondary production [*McClain et al.*, 1996].

Mixed layer depth is regulated by wind stirring, buoyancy forcing via surface heat and freshwater fluxes, and the density jump at the base of the mixed layer [*Alexander et al.*, 2000]. During late winter in the subarctic North Pacific, the mixed layer extends down to the upper portion of the halocline, located between depths of approximately 70 m to 120 m [Fig. 3; *Roden*, 1964; *Freeland et al.*, 1997; *de Boyer Montégut et al.*, 2004]. Thus, low-frequency changes in the Ekman pumping in the Gulf of Alaska, which vertically displaces the halocline, may impact the wintertime MLD. Indeed, after the mid-1970s, the pycnocline was shallower in the central part of the Gulf of Alaska and deeper in a broad band along the coast, primarily due to the local response to Ekman pumping [*Cummins and Lagerloef*, 2002; *Capotondi et al.*, 2005].

Decadal changes in the physical state of the North Pacific Ocean during the 1976 transition and their impact on the phytoplankton and zooplankton were simulated by *Haigh et al.* [2001] and *Chai et al.* [2003] using an ecosystem model embedded in an ocean general circulation model (OGCM). *Haigh et al.* performed simulations for the

years 1952-1975 and for 1977-1989, using the *mean* atmospheric forcing over those two periods. The model reproduced the observed increase in phytoplankton in the central Pacific in summer and a southward displacement of the subtropical chlorophyll front in all seasons in the later period relative to the earl one. The model also indicated an increase in zooplankton over the eastern subarctic Pacific in summer after 1976, but the magnitude and pattern of the increase differed from the observed values in *Brodeur and Ware* [1992]. *Chai et al.* [2003] used *time-dependent* forcing and substantially different physical and biological components than *Haigh et al.* [2001] to investigate variability in the subtropical chlorophyll front. They found that the front expanded and extended farther south after the 1976-77 shift, in agreement with *Haigh et al.*. In the present study, we use the model simulation described by *Chai et. al.* [2003] to investigate the physical and biological changes in the northeast Pacific Ocean, especially those which occurred across the 1976-77 transition.

2. The Model Simulation

The physical component of the model, which simulates temperature, salinity and currents, is the National Center for Atmospheric Research (NCAR) ocean model (NCOM), described by *Large et al.* [1997] and *Gent et al.* [1998]. NCOM is derived from the Geophysical Fluid Dynamics Laboratory (GFDL) Modular Ocean Model with the addition of a mesoscale eddy flux parameterization along isopycnal surfaces [*Gent and McWilliams*, 1990] and a non-local planetary boundary layer parameterization [*Large et al.*, 1994]. The advection of tracers, including temperature, salinity and the biogeochemical components, is calculated using a third-order differencing scheme. The

background horizontal and vertical mixing coefficients for all tracers are 2.0×10^6 cm^{-2} $sec^{-1}$and 0.1 cm^{-2} sec^{-1}, respectively. The version of the model used here, described by *Li et al.* [2001], covers the Pacific from 45°S to 65°N and from 100°E to 70°W with realistic geometry and bathymetry. There is no flow through the boundaries and a sponge layer, where the model's temperature, salinity, nitrate and silicate are relaxed towards observations, is applied within 10° of the meridional boundaries. The longitudinal resolution is a uniform 2°. The latitudinal resolution is 0.5° within 10° of the equator, gradually increases to 2° within 20° of the equator, and is fixed at 2° north of 20°N and south of 20°S. There are 40 vertical levels, with 23 in the upper 400 m. The model's relatively coarse horizontal and vertical resolution allows us to examine basin-scale variability over an extended period of time, but is not sufficient to resolve eddies or coastal processes.

The biological model, developed by *Chai et al.* [2002], consists of ten compartments with two classes of phytoplankton (P1, P2) and zooplankton (Z1, Z2), two forms of dissolved inorganic nitrogen: nitrate (NO_3) and ammonium (NH_4), detrital nitrogen (DN), silicate ($Si(OH)_4$), detrital silicon (DSi), and total carbon dioxide (TCO_2). Small phytoplankton (P1) have variable growth rates, that depends on temperature, nitrogen and light. Their biomass is regulated by micrograzers (Z1), while their net productivity is largely remineralized [*Landry et al.*, 1997]. The large phytoplankton class (P2 > 10 μm) represents the diatom functional group, which can grow rapidly under optimal nutrient conditions [*Coale et al.*, 1996]. Iron and its limitation on phytoplankton growth is not modeled directly but is treated implicitly via two parameters: the slope of the photosynthetic rate over irradiance at low irradiance and the maximum phytoplankton

growth rate [*Chai et al.*, 2002; *Chai et al.*, 2007]. The parameter values, which are constant in space and time, were derived from the limited number of available lab and field experiments, and model simulations of iron addition experiments in the equatorial Pacific (*Chai et al.*, 2007). The micrograzers have growth rates similar to P1 and grazing rates (G1) that depend on the density of both P1 and Z1 [*Landry et al.*, 1997]. The mesozooplankton (Z2) graze on P2 and DN and prey on Z1 and have a feeding threshold based on conventional grazing dynamics [*Frost and Frazen*, 1992]. The loss of Z2 from the system, primarily due to predation from higher trophic levels, is represented by a quadratic expression. Sinking particulate organic matter is converted to inorganic nutrients via regeneration, similar to the process described by *Chai et al.* [1996]. Nitrogen is the "currency" in the ecosystem model, i.e. plankton biomass and detritus pools are in units of millimoles of nitrogen per cubic meter (mmol N m^{-3}). A detailed discussion of the model equations and parameter values is given in *Chai et al.* [2002].

The model's temperature, salinity and nutrients were initialized using climatological values from the National Ocean Data Center (NODC), while the biological components were assigned a value of 0.025 mmol m^{-3} at the surface, decreasing exponentially with a scale length of 120 m – the average depth of the euphotic zone. The full model was then integrated for 10 years with climatological forcing, during which it reached a stable annual cycle in the upper ocean *Chai et al.* [2003]. During this spin-up period and in the subsequent model experiment the physical and ecosystem components were integrated synchronously.

In the simulation examined here, the model is forced with observed atmospheric fields over the period 1955-1999 and the output is archived monthly during 1960-1999,

allowing for a five-year spin-up period. The surface fluxes of momentum, heat, fresh water, and insolation used to drive the model were derived from monthly mean values obtained from the Comprehensive Ocean Atmosphere Data Set [COADS; *da Silva et al.*, 1994] over the period 1955-1993. From 1993-1999 the surface fluxes were obtained from the National Center for Environmental Prediction (NCEP) reanalysis [*Kalnay et al.*, 1996; *Kistler et al.*, 2001]. The heat flux includes shortwave and longwave radiation and the sensible and latent heat flux. The sensible (latent) fluxes are computed using the observed air temperature (specific humidity) and the model's SST. The model does not include the diurnal cycle, so the daily averaged insolation is used for calculating photosynthesis. The model is forced by the observed difference between precipitation and evaporation derived from COADS. Since precipitation is not well measured over the ocean, the salinity of the surface layer is also relaxed to the observed climatological monthly mean values [*Levitus et al.*, 1994] using a 30-day time scale. While this damping greatly reduces the surface salinity variability, the deeper ocean, including the halocline, is relatively unconstrained. *Li et al.* [2001] and *Chai et al.* [2003] provide more detailed descriptions of the procedures used to initialize and force the model and its fidelity in simulating the physical and biological state of the Pacific Ocean.

3. Results

3.1 SST Changes

We will mainly focus on the years 1970-76 and 1977-88 since they were dominated by opposite phases of the PDO [*Bond et al.*, 2003] and because the fields used to force the model during these years were all derived from COADS (NCEP reanalysis is used to

drive the model after 1993). The epoch difference (Δ, defined as 1977-1988 minus 1970-1976 from hereon) in the observed and simulated North Pacific SST (°C) during February-March-April (FMA) is shown in Fig. 1. In both observations and the OGCM, negative ΔSST in the central and western Pacific between approximately 25°N-45°N is ringed by positive ΔSST over the remainder of the North Pacific, indicative of a change to the positive phase of the PDO after 1976. The model also reproduces several of the finer-scale features of the ΔSST field, with negative centers at 30°N, 155°W and 40°N, 175°E, and positive centers in the vicinity of the Alaskan Peninsula and Baja California. The latter is part of a broad swath the extends over much of the tropical Pacific suggesting that the PDO is part of a larger pattern that includes the tropics as well as the North Pacific, consistent with the findings of *Zhang et al.* [1997], *Newman et al.* [2003] and *Deser et al.* [2004]. The close correspondence between the observed and simulated ΔSST fields provides some confidence in the GCM's ability to simulate decadal changes in the northeast Pacific, although using the observed air temperature to compute the surface fluxes partially constrains the SSTs to track observations [e.g. *Seager et al.*, 1995].

3.2 Physical – Biological linkages

A number of studies, including *Brodeur and Ware* [1992], *Polovina et al.* [1995] and *Freeland et al.* [1997], indicated that surface mixing in winter has a strong impact on the Gulf of Alaska ecosystem over the course of the seasonal cycle. The ΔMLD (m) during February-April (FMA) is shown for the GOA (contours) in Fig. 2, where the MLD is defined as the depth where the potential density is 0.125 kg/m^3 greater than the surface

value. The mixed layer shoals by more than 20 m in the central gulf in 1977-1988 relative to 1970-1976, a reduction of ~30%. Unlike in temperate waters where there is a robust inverse relationship between SST and MLD anomalies [e.g. see *Deser et al.*, 1996], the shoaling in the central GOA occurs near the nodal line for decadal SST changes (not shown), and ΔSST and ΔMLD are both positive along the North American coast.

The MLD in Feb and FMA are overlain on the temperature and salinity profiles in FMA from 1960 to 1999 averaged over a region (46°N-52°N, 160°W-140°W, box in Fig. 2) in the central GOA (Fig. 3). The MLD, which extends to the upper portion of the halocline, closely tracks the vertical variations in salinity but not temperature, including the epoch changes in the halocline around 1976. The close correspondence between MLD and the halocline occurs even though the salinity variations near the surface are negligible in the model due to the strong restoring of the surface salinity towards climatology. Furthermore, the epoch difference in salinity, at depths of 70 m to 150 m, closely resemble the MLD pattern, with increased salinity in the center of the gyre and decreased salinity along the coast (not shown). Our results, in conjunction with those of *Cumins and Lagerloef* [2002] and *Capotondi et al.* [2005], suggest that the *wintertime* MLD in the GOA is primarily set by dynamical ocean processes that regulate the depth of the halocline. The shoaling of the halocline and hence the mixed layer in the central GOA, reflects the enhanced Ekman pumping associated with a deeper Aleutian low during 1977-88 relative to 1970-76 [see Fig. 4 in *Capotondi et al.*, 2005].

Changes in MLD can influence primary productivity by regulating the amount of light and nutrients available for photosynthesis. In the northeast Pacific, the highest

primary productivity (PP) during the seasonal cycle, integrated over the upper 100 m of the model, occurs in March-May (see section 3.3). The epoch difference in primary productivity (ΔPP in mmol N m^{-2} day^{-1}) during MAM is also shown in Fig. 2. The ΔPP pattern, with a decrease in the central GOA ringed by an increase along the coast, is remarkably similar to the structure of ΔMLD; indeed the pattern correlation between the two is 0.91.

The positive correlation between MLD and PP initially suggested to us that vertical mixing of nutrients into the surface layer may have been the cause of the simulated biological changes in 1977-88 relative to 1970-76 in the GOA. However, the changes in nutrients do *not* appear to be responsible for the reduction in productivity after 1976, since the patterns of the ΔNO_3 and ΔH_4SiO_4 are quite different than ΔPP (not shown), and the concentrations of both NO_3 and H_4SiO_4 exceed 5 mmol m^{-3} over most of the northeast Pacific during 1977-1988 (not shown), which is sufficient to maintain rapid phytoplankton growth [*Chai et al.*, 2002, 2003].

3.3 MLD, Light Regulation and Trophic Interactions

What is the primary factor linking the epoch difference in MLD with primary productivity in the GOA if it is not a change in (macro) nutrients? One possibility is that changes in MLD impact phytoplankton by altering the light available for photosynthesis, followed by trophic interactions that modify the initial biological response as the seasonal cycle progresses. Specifically, a shoaling of the wintertime MLD in 1977-88 relative to 1970-76 leads to more light and thus enhanced primary productivity and greater phytoplankton biomass earlier in the year in the central GOA region. The resulting

3 increase in phytoplankton enhances the food supply enabling a more rapid rise in the
4 zooplankton biomass, but the associated increase in grazing subsequently suppresses
5 phytoplankton and then zooplankton biomass during their peak in spring.

6 To test this hypothesis we first examine if the epoch changes are coherent across
7 trophic levels and if these changes vary over the seasonal cycle. The 1977-88 mean and Δ
8 in biomass are shown in Fig. 4a-d for each of the four plankton classes over the northeast
9 Pacific. (The mean values during 1977-88 are similar to those from the entire 1960-1999
10 record - not shown). The biomass values (mmol N m^{-3}) are presented during the calendar
11 month in which the mean and Δ peak: March for small phytoplankton (P1), April for
12 microzooplankton (Z1) and large phytoplankton (P2), and May for mesozooplankton
13 (Z2). The biomass shown in Fig. 4 (and from hereon) is obtained from the surface layer
14 (0-10 m) of the model, where the epoch differences are largest. The mean P1 and P2
15 biomass (contours) peaks at ~50°N, while the Z1 and Z2 reach maximum values north of
16 ~52°N.

17 We note that the simulated long-term mean plankton biomass is greater than observed
18 during the warm season, i.e. P is approximately twice that measured at Ocean Weather
19 Station P (50°N, 145°W) during April-June [*Chai et al.*, 2003]. Additionally, spring
20 blooms are not commonly observed in the central GOA [*Boyd and Harrison*, 1999;
21 *Brickley and Thomas*, 2004]. The overabundance of plankton, and P2 in particular, is
22 likely due to the treatment of iron-limited growth in the model, as discussed further in
23 section 4.

24 The Δ biomass for all four plankton classes (shading in Fig. 4) is negative and of
25 large amplitude relative to the mean, indicating a substantial decrease in biomass after

1976. For example, P2 decreases by more than 60% in the vicinity of 46°N, 150°W during April. The reduction in both phytoplankton and zooplankton biomass are collocated and centered within and slightly to the south of the maximum in the long-term mean. The average biomass in the two periods and the difference between them are presented as a function of calendar month for the central GOA region in Fig. 4e and 4f, respectively. The P and Z biomass in the central GOA region decreases by ~40% in 1977-1988 relative to 1970-76 during its spring peak. This decrease is both preceded and followed by an increase in biomass in all four plankton classes, although the increase is relatively small except for P2 and Z2 in March and April, respectively. The spatial coherence of ΔP and ΔZ, and the reversal in sign of the Δ in biomass with month is consistent with our hypothesis that trophic interactions and their evolution over the seasonal cycle play an important role in modulating the low-frequency ecosystem variability.

Given that the magnitude of the mean and the epoch difference in biomass are much greater for the larger plankton classes (Fig. 4), we focus on the dynamics of P2 and Z2 from hereon. The time series of the P2 and Z2 biomass (mmol N m^{-3}) from 1960-1999 averaged over the central Gulf of Alaska region for the months of March, April and May, along with the MLD (m) in March, are shown in Fig. 5. The MLD is well above average during the early epoch, except for 1970 and well below average for later epoch, except for 1977, 1980 and 1982, which are near normal. There is an inverse relationship between MLD and P2 biomass (Fig. 6a) as reflected by a -0.67 correlation between the two over the entire record (significant at the 99% level allowing for autocorrelation in the timeseries, e.g. see *Wilks*, 1995). The phytoplankton biomass in March is below normal

for all years between 1971 and 1976 but it is near normal and has much greater interannual variability during the 1977-88 period, which suggests that the deeper mixed layer during the first period has a greater impact on photosynthesis and phytoplankton biomass than the shallower mixed layer in the later period. The asymmetry in the relationship between MLD and P2 biomass is also indicated by a scatter plot of the two variables averaged over the GOA region during March, where P is nearly independent of MLD for depths < ~65 m (Fig 6a). The existence of a threshold depth, however, is difficult to determine given the scatter in Fig. 6a, i.e. the P2 variability that is unrelated to MLD, and the small number of relatively shallow MLD values.

In winter the phytoplankton and zooplankton biomass are low and vary together in the GOA region (Fig. 5a), e.g. the correlation between P2 and Z2 in March is 0.72. The positive correlation suggests that grazing is not controlling phytoplankton biomass accumlation. While the Z2 biomass is generally low during March, it is nearly zero during 1970-76 (Figs. 4e and 5a). Very low zooplankton abundance in winter can be a critical factor in enabling rapid phytoplankton growth in spring [Fig 6c; *Evans and Parslow*, 1985; *Frost*, 1991; *Fasham*, 1995]. Indeed, the P2 biomass switches from well below normal in March to well above normal in April during 1970-76 (Fig. 5b). The Z2 biomass remains anomalously low in April, reflecting the limited food supply in the previous month. Following the increase in P2 biomass in April, the Z2 biomass in May is above normal during the early 1970s. In contrast to 1970-76, neither P2 nor Z2 exhibit significant changes in the mean during 1977-88; rather, they exhibit large interannual variability.

The lagged P-Z relationships during 1970-1976 in March through May are also very robust over the entire 40-year record, as indicated by the limited scatter between P2 and Z2 (Fig. 6b,c). The P2(Mar)-Z2(Apr) and P2(Apr)-Z2(May) correlations are 0.89 and 0.95, respectively, while the Z2(Mar)-P2(Apr) and Z2(Apr)-Z2(may) correlations are both ~-0.85. The relationship between P2 with Z2 in the following month appears to be linear (Fig. 6b), with a greater change in Z2(Apr) relative to a unit change in P2(Mar) than for Z2(May) relative to P2(Apr). While a linear relationship provides a reasonable fit for Z2(Mar)-P2(Apr) and for Z2(Apr)-P2(May), the two combined suggest a decreasing exponential function (Fig. 6c). The concurrent P2-Z2 correlations in the GOA region are -0.72 and 0.77 in April and May respectively; while significant, the change of sign between months and the slight decrease in magnitude compared to the lag correlations, suggest that the concurrent P-Z correlation values during spring reflect the lag relationship between the two trophic levels. However, we may not be fully resolving the period of the lag with monthly data.

The magnitude of the lead-lag correlations between P and Z at individual grid points generally exceeds 0.4 over the most of the northeast Pacific and 0.6 in the central and western GOA (not shown). Consistent with the regional analyses, the one-month lag P2-Z2 correlations are positive and the Z2-P2 correlations are negative for both March to April and April to May.

The timing of the mixed layer depth and plankton changes with respect to the seasonal cycle are examined further in Fig. 7 using time-latitude (Hovmöller) diagrams of monthly mean (contours) and Δ (shaded) values of a) MLD (m) and b) P2 and c) Z2 biomass (mmol N m^{-3}). The variables are averaged over 160ºW-140ºW and presented for

40°N-57°N from January through July. The maximum mean MLD exceeds 80 m during January-March in the vicinity of 50°N and then decreases at all latitudes to about 20 m by May. The mean P2 biomass begins increasing in mid-winter, reaching a maximum in February, March, and April, for the latitude bands 40°-44°N, 44°-47°N and 48°-57°N, respectively. In addition to the seasonal cycle in insolation, the canonical evolution of P2 also depends on MLD, which is shallower in the southern part of the domain in JFM and thus more conducive for photosynthesis in a light-limited regime. The mean Z2 biomass increases during late winter, peaks in April-May and then declines but much more slowly than P2.

During January-March the Δ P2 biomass increases where the Δ MLD has decreased and vice versa, with the greatest increase in P2, located at 48°N in March, occurring in conjunction with the greatest decrease in MLD (shading, Fig. 7). This inverse relationship between ΔMLD and ΔP2, occurs over most of the domain during winter and is consistent with changes in light limitation influencing phytoplankton growth on decadal time scales. However, this relationship breaks down later in the spring and south of ~46°N in late winter as light is less of a factor in regulating primary productivity and grazing by zooplankton may have already begun to constrain the phytoplankton biomass. As in the central GOA region, ΔP2 and ΔZ2 are enhanced prior to the annual mean peak in winter, reduced during and slightly after the peak in spring, and then weakly enhanced by July between 40°N and 54°N. For example, at 48°N the sharp increase in P2 in March is followed by a rapid rise in Z2 in April, while the decrease in P2 in April is followed by a decrease of Z2 in May.

Primary productivity (PP) of P2 and grazing (G) of P2 by Z2 (mmol N m^{-2} day^{-1}) averaged over the upper 100 m are shown for northeast Pacific during the months of February through May in Fig. 8. The maximum PP averaged over the 1977-88 period (contours) migrates from the southern to the northern edge of the GOA from February to May, as the amount of light necessary for photosynthesis moves northwards. This migration is not zonally uniform, as the largest values occur in the latitude bands 135°W-140°W, 130°W-135°W and 135°W-150°W in Feb, Mar and Apr-May, respectively. The overall maximum mean PP occurs in April rather than June (not shown), suggesting that factors other than the availability of light is limiting phytoplankton growth in late spring and summer. In general, the mean PP and G patterns are very similar, although the latter is shifted south of the former but only by ~2º latitude. The collocation of PP and G is consistent with local grazing on P2 by Z2, since the plankton life cycles occur much faster than the advection by ocean currents. The slight southward displacement of G relative to PP is likely due to the initiation of photosynthesis earlier in the seasonal cycle and thus further north relative to grazing by zooplankton and so the spatial pattern of G in March and April resemble the PP pattern in the previous month.

Like the mean values, the ΔPP and ΔG (shading in Fig. 8) also move northward across the GOA from February to May and the grazing is shifted slightly south relative to the primary productivity. ΔPP and ΔG are generally positive to the north and negative to the south of their respective maximum in the 1977-88 mean values, indicating a northward displacement in biological activity after the 1976 regime shift. The epoch differences are also a substantial fraction of the mean, e.g. primary productivity decreased by as much as ~70% in 1977-1988 relative to 1970-1976. There is generally a

close correspondence between the ΔPP and ΔG for each calendar month. Thus, there is both enhanced PP and G over much of the Alaskan gyre during February through April after 1976. The increase in grazing is especially pronounced between 48°N-52°N and 145°W-155°W in March and April, and likely contributes to the strong suppression of PP in May in the central GOA.

4. Summary and Conclusions

We have used a physical-ecosystem model to examine whether changes in the physical environment associated with the 1976-77 transition influenced the lower trophic levels of the food web and if so by what means. We hypothesize the following chain of events lead to the difference in the physical climate and biology in the central Gulf of Alaska in 1977-88 relative to 1970-76 in the model. The Aleutian Low strengthened [e.g. *Trenberth and Hurrell*, 1994] and the associated cyclonic winds accelerated the Alaskan gyre and enhanced Ekman pumping [*Capotondi et al.*, 2005]. The resulting increase in upwelling caused the halocline to shoal in the center of the Alaskan Gyre. Thus the mixed layer, which extends to the upper portion of the halocline in winter, did not penetrate as deep. As a result, more phytoplankton remained in the euphotic zone and primary productivity and phytoplankton biomass increased earlier in spring. The enhanced food supply led to an increase in zooplankton biomass but then grazing pressure led to a strong (~40%) decrease in phytoplankton by April followed by a reduction in zooplankton by May. The one-month lag between P and Z in spring likely reflects the timescales set by photosynthesis and grazing, although this was based on monthly averaged data and does not consider all of the potential biological interactions in the system such as nutrient

recycling (see Fig. 1). Finally, there was a modest rebound in plankton concentrations by mid summer, but the magnitude of the simulated increase (~10%) over the GOA was substantially smaller than the observed doubling in zooplankton biomass [*Brodeur and Ware*, 1992].

The results presented here are dependent on the simulation of variability in both the physical and biological models. As in previous studies the winter mixed layer depth appears to be a critical variable for ecosystem dynamics in the North Pacific. Decadal variability of MLD in the northeast Pacific depends on dynamical ocean processes that influence the density jump at the base of the mixed layer (and top of the halocline). Interannual and decadal changes in MLD and phytoplankton biomass in the GOA are inversely related, indicative of a light regulated ecosystem as suggested by [*Boyd et al.*, 1995, *Polovina et al.*, 1995], but *only* during winter. Subsequent changes in grazing rates appear to cause larger changes in biomass during their spring peak, leading to a positive correlation between winter MLD and spring primary productivity/plankton biomass. The importance of grazing in regulating the spring plankton biomass in the northeast Pacific has been noted before in the context of the mean seasonal cycle using one-dimensional models [*Evans and Parslow*, 1985; *Frost* 1991; *Fasham*, 1995] and a three-dimensional physical/biogeochemical model [*Gregg*, 2002]. The epoch differences in biomass can also be viewed as changes in the seasonal cycle with the spring transition, or alternatively the northward seasonal advance of primary and secondary production, beginning earlier in the year in 1977-88 relative to 1970-76. *Mackas et al.* [1988], *Stabeno and Overland* [2001] and *Bograd et al.* [2002] have also found that decadal variability in the North Pacific climate and ecosystems can be manifest in the seasonal cycle.

Based on previous analyses [e.g. *Bond et al.*, 2003] and the simulation of SST in the OGCM, we selected 1970-76 and 1977-88 as periods that exhibited "regime-like" behavior, i.e. when anomalies are of one sign. This appeared to be a fairly reasonable assumption for MLD depth, which is shallow (deep) during 1977-88 (1970-76) in the central GOA. However, the biological anomalies were consistent in sign only for 1970-76; during 1977-88 phytoplankton and zooplankton biomass were close to their long-term means and exhibited substantial interannual variability. The reason for this difference between periods is unclear, although it may be due to a nonlinear relationship between MLD and primary productivity, i.e. the phytoplankton is much more sensitive to changes in the March MLD, when the latter exceeds ~65 m in the GOA region. Perhaps when the MLD is less than a given depth enough light is available to sustain phytoplankton growth and it is thus not a strong controlling factor. The high degree of interannual variability during the later period also has important implications for assessing regimes based on observations: insufficient sampling could lead to inaccurate estimates of the actual mean value over a given period.

The model used in the present study may not adequately represent several potentially important processes, including eddies, near-shore processes such as coastally trapped waves, and zooplankton behavior and their interactions with higher trophic levels. In addition, the eastern subarctic Pacific is a high-nutrient, low-chlorophyll (HNLC) region where micronutrients, especially iron, are believed to limit the growth of phytoplankton in late spring and summer [*Martin and Fitzwater*, 1988; *Boyd et al.*, 1996; *SERIES*, 2006). The model's implicit treatment of iron limitation may be adequate for the equatorial Pacific [*Chai et al.*, 2002, 2007], but appears too weak in the northeast Pacific.

This may have lead to an overestimate of the simulated change in primary productivity and plankton biomass in response to the physical changes in the system. However, the processes identified here are still likely to play an important role in decadal variability in the GOA, since the lack of sunlight in conjunction with low iron levels may co-limit growth in winter [*Maldanado et al.*, 1999], and grazing in combination with the limited iron supply may modulate spring blooms [*Frost*, 1991; *Fasham*, 1995; *Aumont et al.*, 2003]. While the direct simulation of the iron cycle has recently been included in OGCMs [*Aumont et al.*, 2003; *Gregg et al.*, 2003; *Moore et al.*, 2004], several key processes that influence iron cycling in the marine environment are poorly known and thus crudely parameterized. Questions remain regarding the bioavailability, cellular quotas and abiotic scavenging of iron and the magnitude of its external sources [*Johnson et. al.* 1997; *Fung et al.*, 2002; *Johnson et al.*, 2002]. Thus, the role of iron-limitation and small scale/coastal processes upon decadal variability in the North Pacific Ocean warrants further exploration.

Acknowledgements

We thank James Scott for his assistance in processing the data and drafting the figures and Yi Chao and collaborators for developing the OGCM and sharing the output with us. Comments from Hal Batchelder helped to improve the manuscript. This research received financial support from the NOAA office of Polar Programs, NASA's IDS program and the NSF Oceans program.

References

Alexander, M. A., J. D. Scott, and C. Deser (2000), Processes that influence sea surface temperature and ocean mixed layer depth variability in a coupled model, *J. Geophys. Res.*, *105*, 16,823-16,842.

Aumont, O., E. Maier-Reimer, S. Blain and P. Monfray (2003), An ecosystem model of the global ocean including Fe, Si, P colimitations. *Global Biogeochem. Cycles*, *17*, doi:10.1029/2001GB001745.

Benson, A. J., and A. W. Trites (2002), Ecological effects of regime shifts in the Bering Sea and eastern North Pacific Ocean, *Fish and Fisheries, 3*, 95-113.

Bond, N. A., J. E. Overland, M. Spillane, and P. Stabeno, (2003), Recent shifts in the state of the North Pacific, *Geophys. Res. Lett., 30*, 2183.

Bograd, S., F. Schwing, R. Mendelssohn, and P. Green-Jessen, (2002), On the changing seasonality over the North Pacific, *Geophys. Res. Lett.*, *29*, doi:10.1029/2001GL013790.

Boyd, P., and P. J. Harrison (1999), Phytoplankton dynamics in the NE subarctic Pacific. *Deep-Sea Res. II*, 46, 2405-2432.

Boyd, P. W., F. A. Whitney, and P. J. Harrison (1995), The NE subarctic Pacific in winter. 2. Biological rate processes, *Mar. Ecol. Prog. Ser.*, *128*, 25-34.

Boyd, P. W., D. L. Muggli, D. E. Varela, R. H. Goldblatt, R. Chretien, K. J. Orians, and P. J. Harrison (1996), In vitro iron enrichment experiments in the NE subarctic Pacific, *Mar. Ecol. Prog. Ser., 136*, 179–193.

de Boyer Montégut, C., G. Madec, A. S. Fischer, A. Lazar, and D. Iudicone (2004), Mixed layer depth over the global ocean: an examination of profile data and a profile-based climatology, *J. Geophys. Res., 109*, C12003, doi:10.1029/2004JC002378.

Brickley P. J., and A. C. Thomas (2004), Satellite-measured seasonal and interannual chlorophyll variability in the Northeast Pacific and Coastal Gulf of Alaska, *Deep-Sea Res. II*, *51*, 229-245.

Brodeur, R. D., and D. M. Ware (1992), Long-term variability in zooplankton biomass in the subarctic Pacific Ocean, *Fish. Oceanogr.*, *1*, 32-38.

Brodeur, R. D., B. W. Frost, S. R. Hare, R. C. Francis, and W. J. Ingraham (1996). Interannual variations in zooplankton biomass in the Gulf of Alaska and covariation with California Current zooplankton biomass, *CalCOFI Report*, *37*, 80-99.

Capotondi, A., M. A. Alexander, C. Deser, and A. J. Miller (2005), Low frequency pycnocline variability in the northeast Pacific, *J. Phys. Oceanogr.*, *35*, 1403-1420.

Chai, F., R. T. Barber, and S. T. Lindley (1996), Origin and maintenance of high nutrient condition in the equatorial Pacific, *Deep-Sea Res. II*, *42*, 1031-1064.

Chai, F., R. C. Dugdale, T.-H. Peng, F. P. Wilkerson, and R. T. Barber (2002). One-dimensional ecosystem model of the equatorial Pacific upwelling system. Part I: model development and silicon and nitrogen cycle, *Deep-Sea Res. Pt II*, *49*, 2713-2745.

Chai, F., M. Jiang, R. T. Barber, R. C. Dugdale, and Y. Chao (2003), Interdecadal variation of the transition zone chlorophyll front: A physical-biological model simulation between 1960 and 1990*, J. Oceanogr.*, *59*, 461-475.

Chai, F., M.-S. Jiang, Y. Chao, R.C. Dugdale, F. Chavez, and R.T. Barber (2007), Modeling Responses of Diatom Productivity and Biogenic Silica Export to Iron Enrichment in the Equatorial Pacific Ocean. *Global Biogeochemical Cycle*, in press.

Coale, K. H. et al. (1996), A massive phytoplankton bloom induced by an ecosystem-scale iron fertilization experiment in the equatorial Pacific Ocean. *Nature*, *838*, 495-501.

Cummins, P. F., and G. S. Lagerloef (2002), Low frequency pycnocline depth variability at station P in the northeast Pacific, *J. Phys. Oceanogr.*, *32*, 3207-3215.

Da Silva, A. M., C. C. Young-Molling, and S. Levitus, (1994), Atlas of Surface Marine Data: Vol. 1: Algorithms and Procedures. In *NOAA Atlas NESDIS 6*, p 83. U.S. Gov. Printing Office.

Deser, C., M. A. Alexander, and M. S. Timlin (1996), Upper ocean thermal variations in the North Pacific during 1970 – 1991, *J. Climate*, *9*, 1841-1855.

Deser, C., M. A. Alexander, and M. S. Timlin (1999), Evidence for wind-driven intensification of the Kuroshio Current Extension from the 1970s to the 1980s, *J. Climate*, *12*, 1697-1706.

Deser C., A. S. Phillips, and J. W. Hurrell, (2004), Pacific interdecadal climate variability: linkages between the tropics and the North Pacific during boreal winter since 1900, *J. Climate*, *17*, 3109–3124.

Evans, T. G., and J. S. Parslow (1985), A model of annual plankton cycles, *Biological Oceanogr., 3*, 327-347.

Fasham, M. J. R. (1995), Variations in the seasonal cycle of biological production in subarctic oceans: A model sensitivity analysis, *Deep-Sea Res., 42*, 1111-1149.

Freeland, H., K. Denman, C. S. Wong, F. Whitney, and R. Jacques (1997), Evidence of change in the winter mixed layer in the Northeast Pacific Ocean, *Deep-Sea Res.*, *44*, 2117-2129.

Frost, B. W. (1991), The role of grazing in nutrient-rich areas of the open sea, *Limnol. Oceanogr.*, *36*, 1616-1630.

Frost, B. W., and N. C. Frazen (1992), Grazing and iron limitation in the phytoplankton stock and nutrient concentration: a chemostat analogue of the Pacific equatorial upwelling zone*, Mar. Ecol. Prog. Ser.*, *83*, 291-303.

Francis, R. C., S. R. Hare, A. B. Hollowed, and W. S. Wooster (1998), Effects of interdecadal climate variability on the oceanic ecosystems of the NE Pacific. *Fish. Oceanogr.*, *7*, 1-21.

Fung, I. Y., S. K. Meyn, I. Tegen, S. C. Doney, J. G. John, and J. K. B. Bishop (2000), Iron supply and demand in the upper ocean, *Global Biogeochem. Cycles*, *14*, 281-295.

Gargett, A. E. (1997), The optimal stability 'window': a mechanism underlying decadal fluctuations in North Pacific salmon stocks?, *Fish. Oceanogr.*, *6*, 109-117.

Gent, P. R., and J. C. McWilliams (1990), Isopycnal mixing in ocean circulation models. *J. Phys. Oceanogr.*, *20*, 150-55.

Gent, P. R., F. O. Bryan, G. Danabasoglu, S. Doney, W. R. Holland, W. G., Large, and J. C. McWilliams, (1998), The NCAR Climate System Model global ocean component, *J. Climate*, *11*, 1287-306.

Gregg, W. W. (2002), Tracking the SeaWiFS record with a coupled physical/biogeochemical/radiative model of the Global Oceans, *Deep-Sea Res. II*, *49*, 81-105.

Graham, N. E. (1994), Decadal-scale climate variability in the tropical and North Pacific during the 1970s and 1980s: observations and model results, *Climate Dyn.*, *6*, 135-162.

Graham, N. E., T. P. Barnett, R. Wilde, M. Ponater, and S. Schubert (1994), On the roles of Tropical and mid-latitude SSTs in forcing interannual to interdecadal variability in the winter Northern Hemisphere circulation. *J. Climate*, 7, 1416-1441.

Haigh, S. P., K. L. Denman, and W. W. Hsieh, (2001), Simulation of the planktonic ecosystem response to pre- and post-1976 forcing in an isopycnic model of the North Pacific, *Can. J. Fish. Aquat. Sci.*, *58*, 703-722.

Hare, S. R., and N. J. Mantua (2000), Empirical evidence for North Pacific regime shifts in 1977 and 1989, *Prog. Oceanogr., 47*, 103-145.

Jiang, M.-S., F. Chai, R. T. Barber, R. C. Dugdale, F. Wilkerson, and T.-H. Peng (2003), A nitrate and silicate budget in the Equatorial Pacific Ocean: A coupled biological-physical model study. *Deep Sea Res. II*, *50*, 2971-2996.

Johnson, K. S., R. M. Gordon, and K. H. Coale (1997), What controls dissolved iron concentrations in the world Ocean? *Mar. Chem.*, *57*, 137-161.

Johnson, K. S., J. K. Moore and W. O. Smith (2002), Workshop highlights iron dynamics in ocean carbon cycle*, EOS Trans., AGU*, *83*, 481.

Kalnay, E. and Coauthors. (1996), The NCEP/NCAR 40-year reanalysis project, *Bull. Amer. Metor. Soc.*, *77*, 437-71.

Kistler, R., E. Kalnay, W. Collins, S. Saha, G. White, J. Woollen, M. Chelliah, W. Ebisuzaki, M. Canamitsu, V. Kousky, H. van den Dool, R. Jenne and Fiorinio, M. (2001), The NCEP-NCAR 50-year reanalysis: Monthly Means CD-ROM and documentation, *Bull. Amer. Meteor. Soc.*, *82*, 247-67.

Landry, M. R., R. T. Barber, R. R. Bidigare, F. Chai, K. H. Coale, H. G. Dam, M. R. Lewis, S. T. Lindley, J. J. McCarthy, M. R. Roman, D. K. Stoecker, P. G. Verity, and J. R. White (1997), Iron and Grazing Constraints on Primary Production in the Central Equatorial Pacific: An EQPAC Synthesis, *Limnol. Oceanogr.*, *42*, 405-418.

Large, W. C., J. C. McWilliams, and S. C. Doney (1994). Oceanic vertical mixing: a review and a model with a nonlocal boundary layer parameterization, *Rev. Geophys.*, *32*, 363-404.

Large, W. G., G. Danabasoglu, S. C. Doney, and J. C. McWilliams, (1997), Sensitivity to surface forcing and boundary layer mixing in a global ocean model: Annual mean climatology, *J. Phys. Oceanogr.*, *27*, 2418-2447.

Levitus, S., R. Burgett, and T. P. Boyer (1994), NOAA Atlas NESDIS 4; World Ocean Atlas 1994 Volume 3: Salinity. In, Vol. 3. National Oceanic and Atmospheric Administration, Washington, D.C., U.S. Government Printing Office, 99 pp.

Li, X., Y. Chao, J. C. McWilliams, and L.-L. Fu (2001), A comparison of two vertical-mixing schemes in a Pacific Ocean general circulation model*, J. Phys. Oceanogr.*, *14*, 1377-1398.

Mackas, D. L., R. Goldblatt, and A. G. Lewis (1998), Interdecadal variation in developmental timing of *Neocalanus plumchrus* populations at Ocean Station P in the subarcic Pacific, *Can. J. Fish. Aquat. Sci.*, *55*, 1878-1893.

Maldonado, M. T., P. T. Boyd, P. J. Harrison, and N. P. Price, (1999), Co-limitation of phytoplankton by light and Fe during winter in the subarctic Pacific Ocean, *Deep-Sea Res., II*, *46*, 2475-2485.

Mann, K.H. (1993), Physical oceanography, food chains and fish stocks: a review, *ICES, J. Mar. Sci.*, *50*, 105-119.

Mantua, N. J., S. R. Hare, Y. Zhang, J. M. Wallace, and R. C. Francis, (1997), A Pacific interdecadal climate oscillation with impacts on salmon production, *Bull. Amer. Meteor. Soc.*, *78*, 1069-1079.

Martin, J. H., and S. E. Fitzwater (1988), Iron deficiency limits phytoplankton growth in the northeast Pacific subarctic, *Nature*, *331*, 341-343.

McClain C. R., K. Arrigo, K.-S. Tai, and D. Turk (1996), Observations and simulations of physical and biological processes at ocean weather station P, 1951-1980, *J. Geophys. Res.*, *101*, 3697-3713.

McFarlane, G. A. and R. J. Beamish, (1992), Climatic influence linking copepod production with strong year-class in sablefish, *Anoplopoma fimbria*, *Can. J. Fish. Aquat. Sci.*, *49*, 743-53.

Miller, A. J., D. R. Cayan, T. P. Barnett, N. E. Graham, and J. M. Oberhuber (1994), Interdecadal variability of the Pacific Ocean: model response to observed heat flux and wind stress anomalies, *Climate Dyn.*, *10*, 287-302.

Miller, A. J., F. Chai, S. Chiba, J. R. Moisan, and D. J. Neilson (2004), Decadal-scale climate and ecosystem interactions in the North Pacific Ocean, *J. Oceanogr.*, *60*, 163-188.

Moore, J. K., S. C. Doney, and K. Lindsay (2004), Upper ocean ecosystem dynamics and iron cycling in a global three-dimensional model, *Global Biogeochem. Cycle*s. doi:10.1029/2004GB002220.

Newman, M., G. P. Compo, and M. A. Alexander (2003), ENSO-forced variability of the Pacific Decadal Oscillation, *J. Climate*, *16*, 3853-3857.

Polovina, J.J., G. T. Mitchum, N. E. Graham, M. P. Craig, E. E. DeMartini, and E. N. Flint (1994), Physical and biological consequences of a climate event in the central North Pacific. *Fish. Oceanogr.*, *3*, 15-21.

Polovina, J.J., G. Mitchum, and G. T. Evans (1995), Decadal and basin scale variation in mixed layer depth and the impact on biological production in the central and North Pacific, 1960-1988, *Deep-Sea Res., 42*, 1701-1716.

Roden, G. I. (1964), Shallow temperature inversions in the Pacific Ocean. *J. Geophys. Res.*, *69*, 2899-2914.

Rand, P. S., and S. G. Hinch (1998), Spatial patterns of zooplankton biomass in the northeast Pacific Ocean, *Mar. Ecol. Prog. Ser., 171*, 181-186.

Seager, R., Y. Kushnir, and M. A. Cane (1995), On heat flux boundary conditions for ocean models. *J. Phys. Oceanogr.*, *25*, 3219-3230.

Stabeno, P. J., and J. E. Overland (2001), The Bering Sea shifts towards an earlier spring transition. *Eos Trans., AGU, 82*, 317-321.

Steele, J. H., and E. W. Henderson (1993), The significance of interannual variability. In *Towards a model of ocean biogeochemical processes.* G.T. Evans and M.J.R. Fasham editors, NATO ASI series, *1*, pp. 237-260.

Sugimoto, T., and K. Tadokoro (1997), Interannual-interdecadal variations in zooplankton biomass, chlorophyll concentration and physical environment in the subarctic Pacific and Bering Sea, *Fish. Oceanogr.*, *6*, 74-93.

Subarctic Ecosystem Response to Iron Enrichment Study (Series, 2006), Deep Sea Res. II, *53*, Issues 20-22, 2006-2453.

Trenberth, K. E. (1990), Recent observed interdecadal climate changes in the Northern Hemisphere, *Bull. Amer. Meteor. Soc.*, *71*, 988-993.

Trenberth, K. E., and J. W. Hurrell (1994), Decadal atmosphere-ocean variations in the Pacific, *Climate Dyn.*, 9, 303-319.

Venrick, E. L., J. A. McGowan, D. R. Cayan, and T. L. Hayward (1987), Climate and chlorophyll a: long-term trends in the central North Pacific Ocean, *Science*, *238*, 70-72.

Vimont, D. J., D. S. Battisti, and A. C. Hirst (2002), Pacific interannual and interdecadal equatorial variability in a 100-year simulation of the CSIRO coupled general circulation model, *J. Climate*, *15*, 160-78.

Wilks, D. S. (1995), *Statistical Methods in the Atmospheric Sciences*, Academic Press. New York, 454, pp.

Zhang, Y., J. M. Wallace, and D. S. Battisti (1997), ENSO-like interdecadal variability, *J. Climate*, *10*, 1004-1020.

Figure Captions

Fig. 1. The epoch difference, 1977-88 – 1970-76 (Δ), in SST (°C) during January, February, March (JFM) from a) observations and b) the model simulation. The observed values are from COADS.

Fig. 2. The ΔMLD (m) (contours) and ΔPP (in N m^{-2} day^{-1}) averaged over the upper 150 m of the ocean during JFM. The PP values can be converted from units of nitrogen to units of carbon by multiplying them by 6.625 as indicated by the Redfield ratio. Values have been spatially smoothed using a 9-point filter. The box indicates the central Gulf of Alaska (GOA) region.

Fig. 3. The a) temperature (°C) and b) salinity (ppt) over the upper 120 m of the ocean during FMA in the central GOA region (46°N-52°N, 160°W-140°W) for the years 1960-1999. The MLD during February and FMA are shown by an open square and closed circle, respectively.

Fig. 4. The 1977-88 mean (contours) and Δ (shading) for a) small phytoplankton (P1) in March, b) large phytoplankton (diatoms, P2) in April, c) microzooplankton (Z1) in April and d) mesozooplankton (Z2) in May. Also shown are the values of P1, P2, Z1, Z2 for each calendar month for the periods e) 1970-76 and 1977-88, and f) Δ, the difference between the two periods. The P and Z values (mmol N m^{-3}) presented here and the subsequent figures are from the top model level.

Fig. 5. The P2 and Z2 biomass (mmol N m^{-3}) from 1960-1999 averaged over the central Gulf of Alaska region for the months of a) March, b) April and c) May, along with the MLD (m, scale on right axis) in a) March. Also shown are the MLD, P2 and Z2 means (thin lines) over the 1960-1999 period.

Fig. 6. Scatter plot of a) MLD (March) with P2 (April), b) P2 (March) with Z2 (April) and P2 (April) with Z2 (May), c) Z2 (March) with P2 (April) and Z2 (April) with P2 (May). MLD (m) and P2 and Z2 (mmol N m^{-3}) values are for the central GOA region for the years 1960-99. Correlation (r) values between the variables are also given.

Fig. 7. Hovmöller (latitude-time) diagrams of the 1977-88 mean (contours) and Δ (shaded) values of a) MLD (m), b) P2 (mmol N m^{-3}) and c) Z2 (mmol N m^{-3}). The values are averaged over 160ºW-140ºW and shown for January through July.

Fig. 8. The 1977-88 mean (contours) and Δ (shaded) P2 primary productivity (left column) and grazing of P2 by Z2 (right column) for the months of February, March, April, and May. The values have been averaged over the upper 150 m and are in units of mmol N m^{-2} day^{-1}.

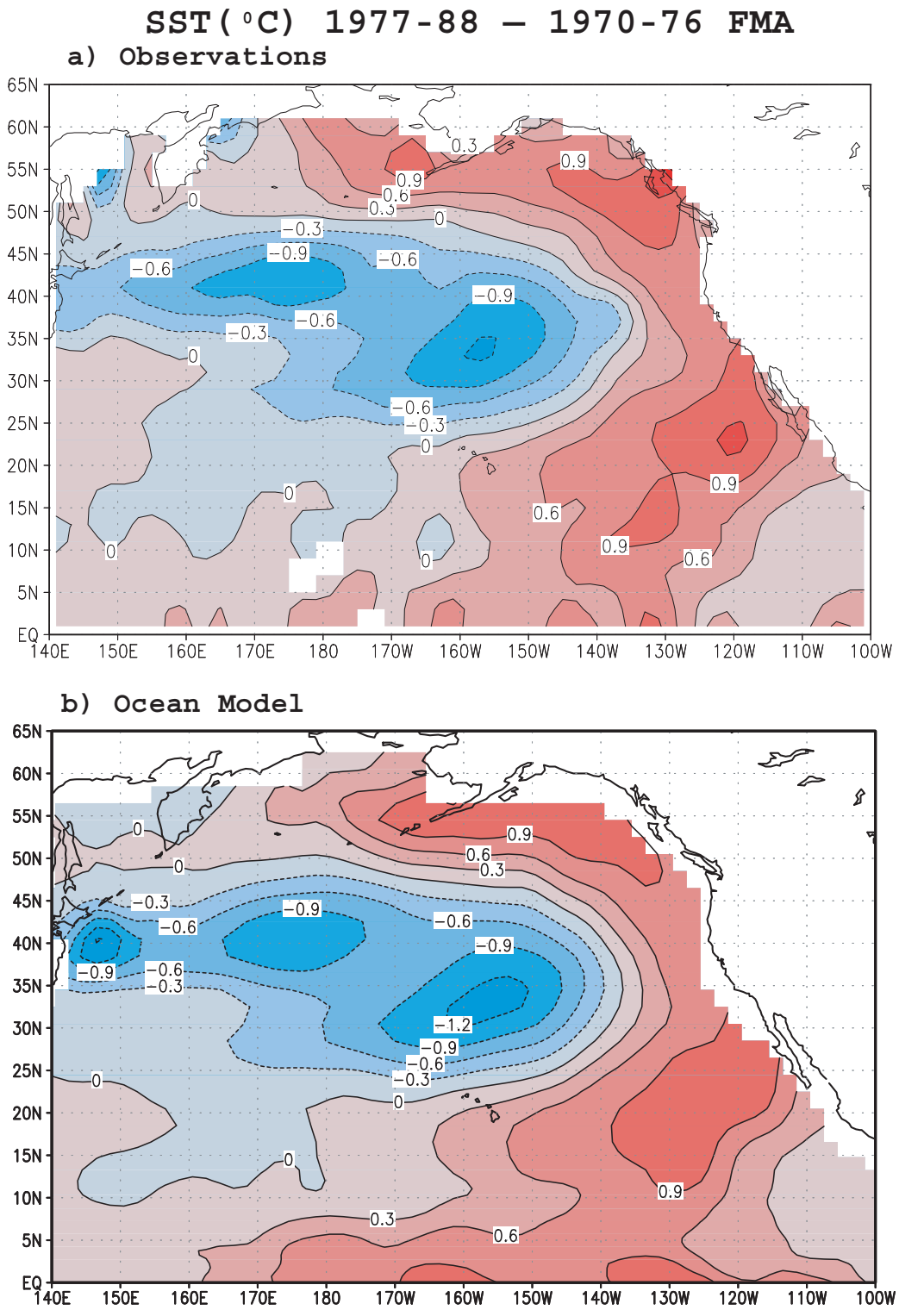

Fig. 1. The epoch difference, 1977-88 - 1970-76 (Δ), in SST (°C) during January, February, March (JFM) from a) observations and b) the model simulation. The observed values are from COADS.

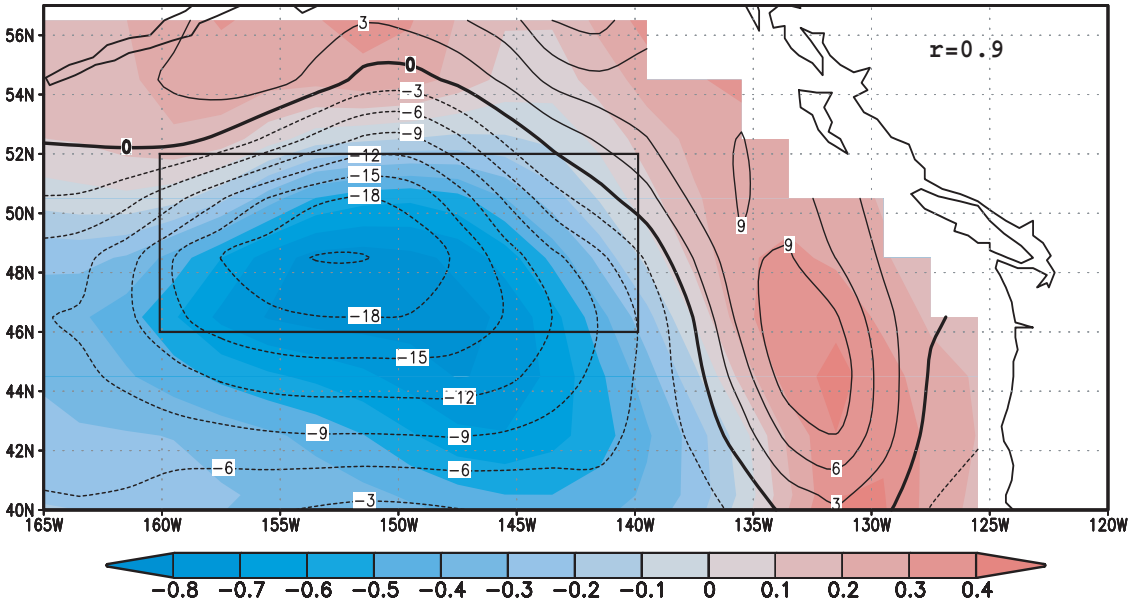

Fig. 2. The ΔMLD (m) (contours) and ΔPP (in N m^{-2} day^{-1}) averaged over the upper 150 m of the ocean during JFM. The PP values can be converted from units of nitrogen to units of carbon by multiplying them by 6.625 as indicated by the Redfield ratio. Values have been spatially smoothed using a 9-point filter. The box indicates the central Gulf of Alaska (GOA) region.

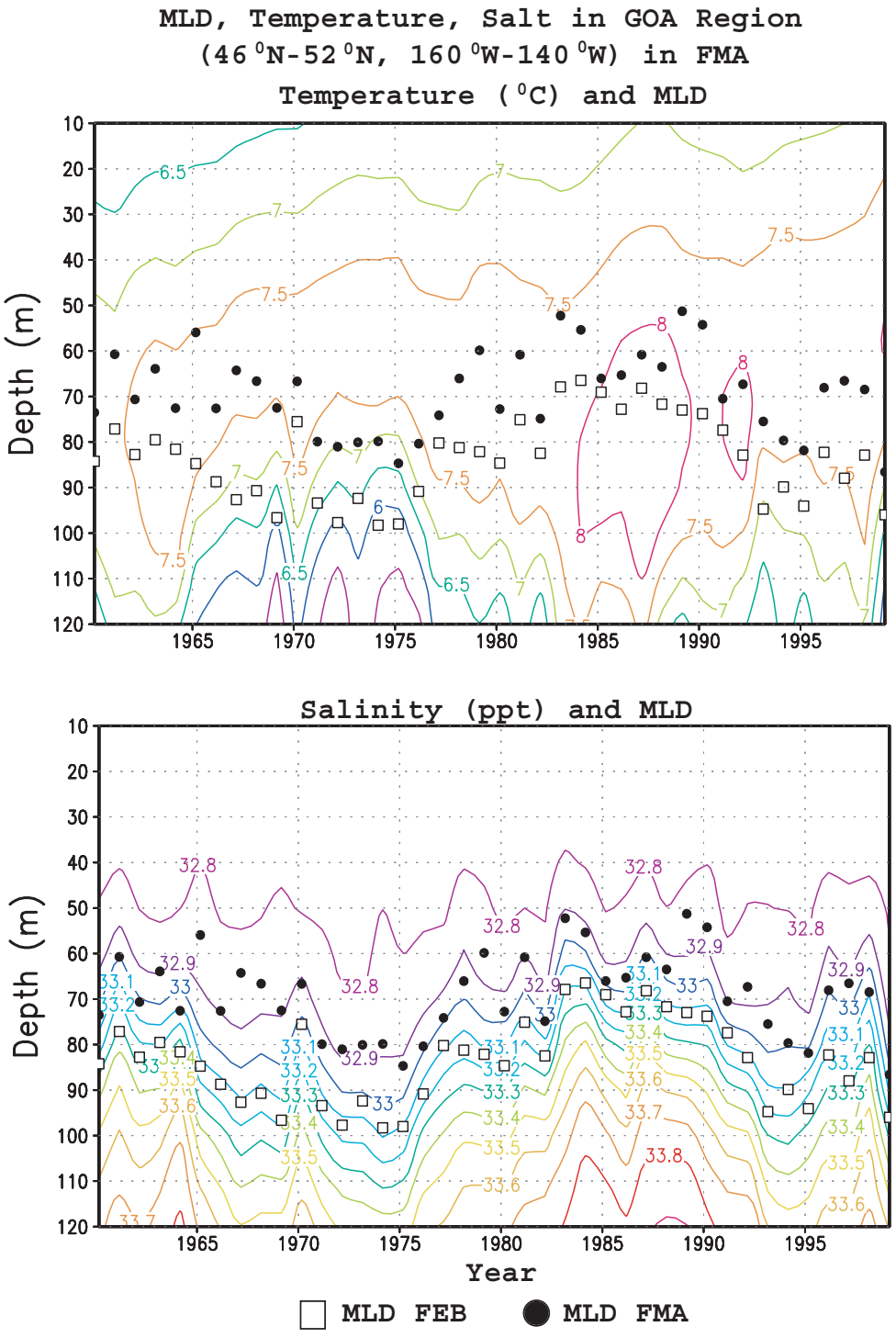

Fig. 3. The a) temperature (°C) and b) salinity (ppt) over the upper 120m of the ocean during FMA in the central GOA region (46°N-52°N, 160°W-140°W) for the years 1960-1999. The MLD during February and FMA are shown by an open square and closed circle, respectively.

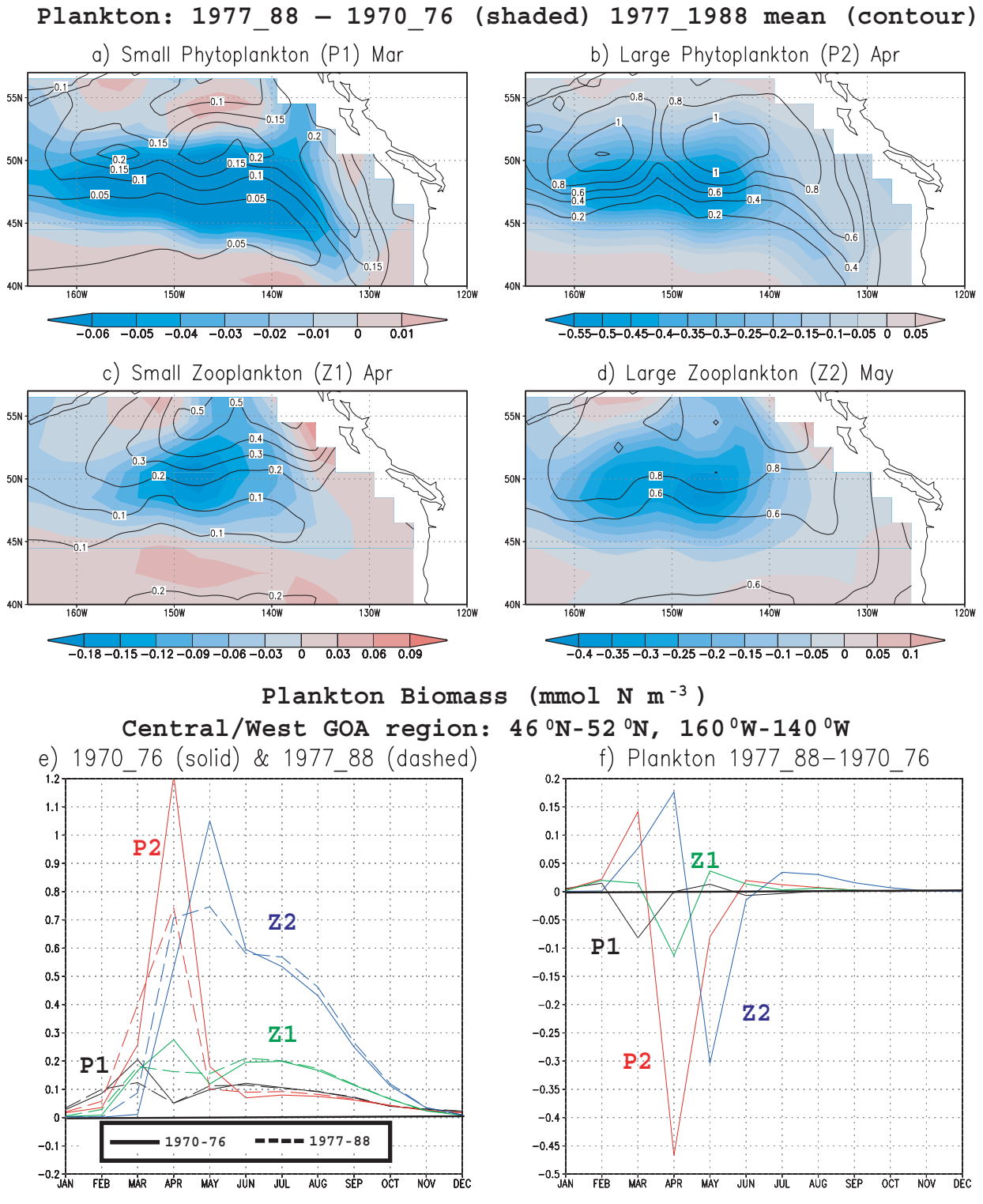

Fig. 4. The 1977-88 mean (contours) and Δ (shading) for a) small phyto-plankton (P1) in March, b) large phytoplankton (diatoms, P2) in April, c) microzooplankton (Z1) in April and d) mesozooplankton (Z2) in May. Also shown are the values of P1, P2, Z1, Z2 for each calendar month for the periods e) 1970-76 and 1977-88, and f) Δ, the difference between the two periods. The P and Z values (mmol N m^{-3}) presented here and the subsequent figures are from the top model level.

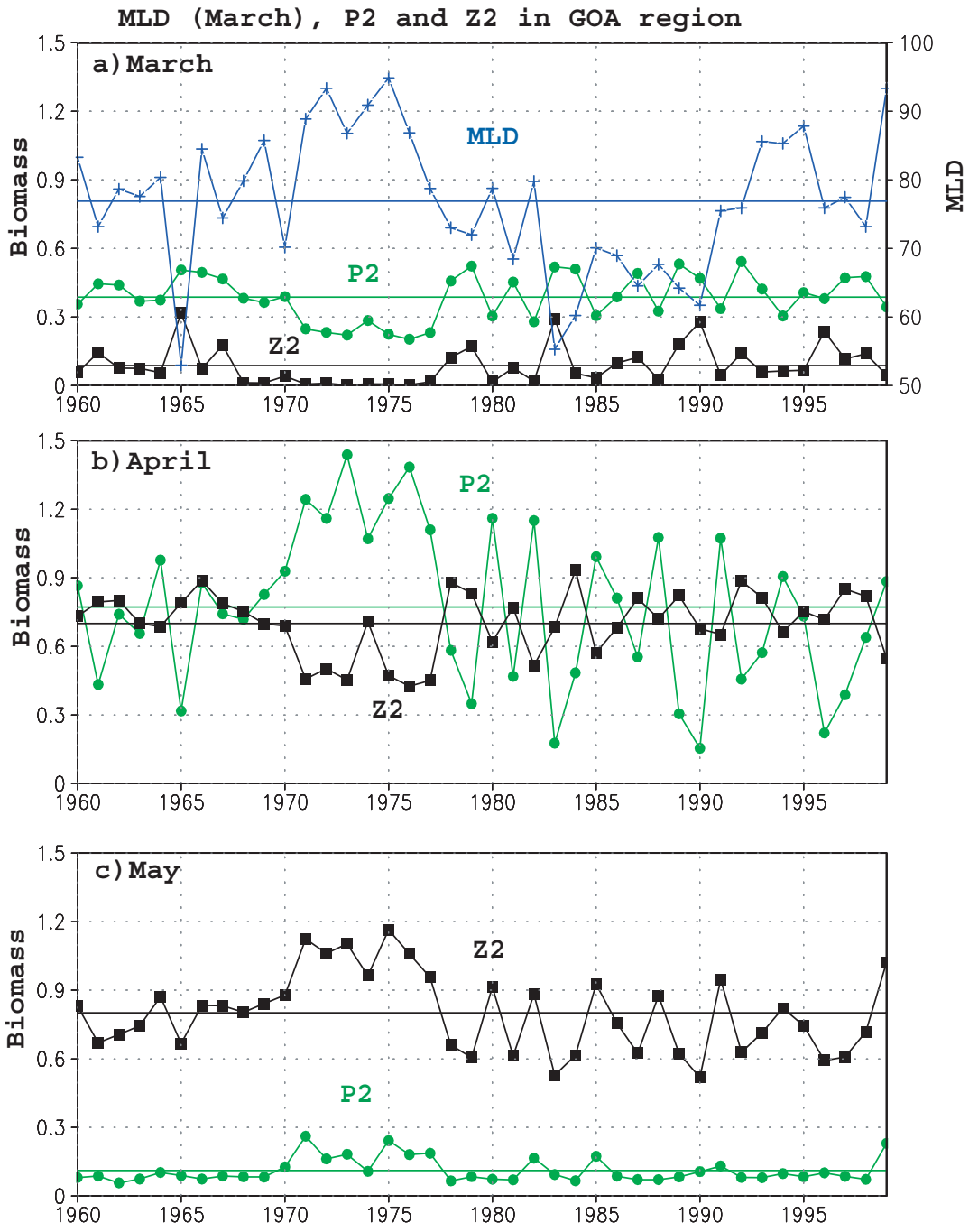

Fig. 5. The P2 and Z2 biomass (mmol N m^{-3}) from 1960-1999 averaged over the central Gulf of Alaska region for the months of a) March, b) April and c) May, along with the MLD (m, scale on right axis) in a) March. Also shown are the MLD, P2 and Z2 means (thin lines) over the 1960-1999 period.

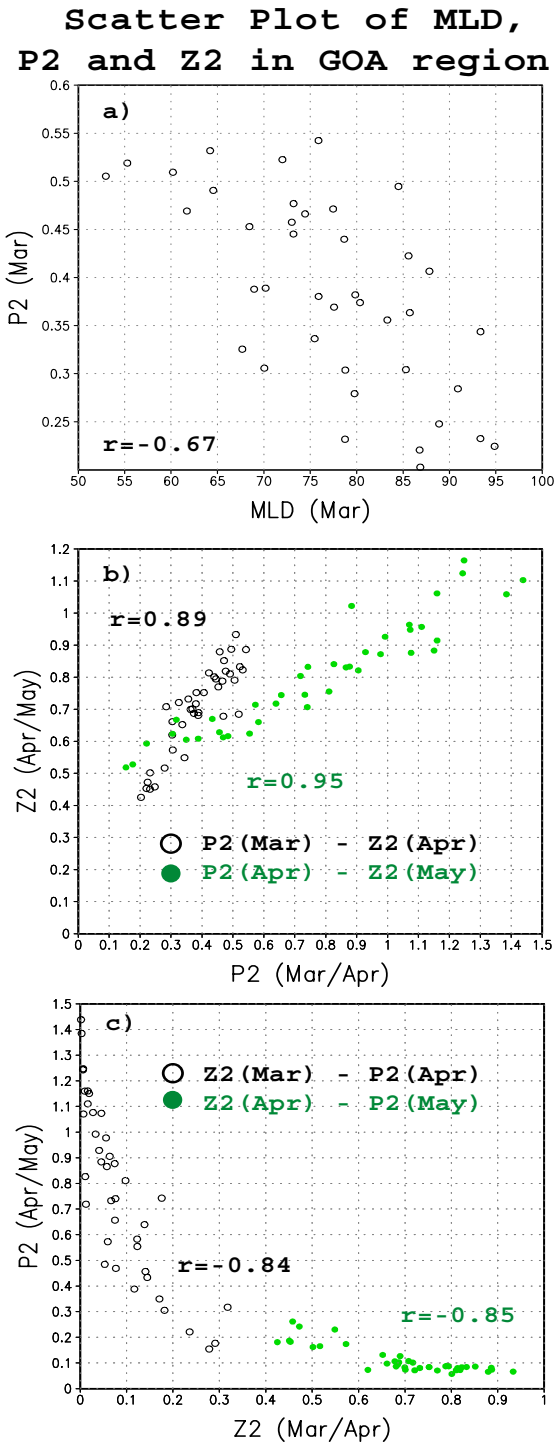

Fig. 6. Scatter plot of a) MLD (March) with P2 (April), b) P2 (March) with Z2 (April) and P2 (April) with Z2 (May), c) Z2 (March) with P2 (April) and Z2 (April) with P2 (May). MLD (m) and P2 and Z2 (mmol N m^{-3}) values are for the central GOA region for the years 1960-99. Correlation (r) values between the variables are also given.

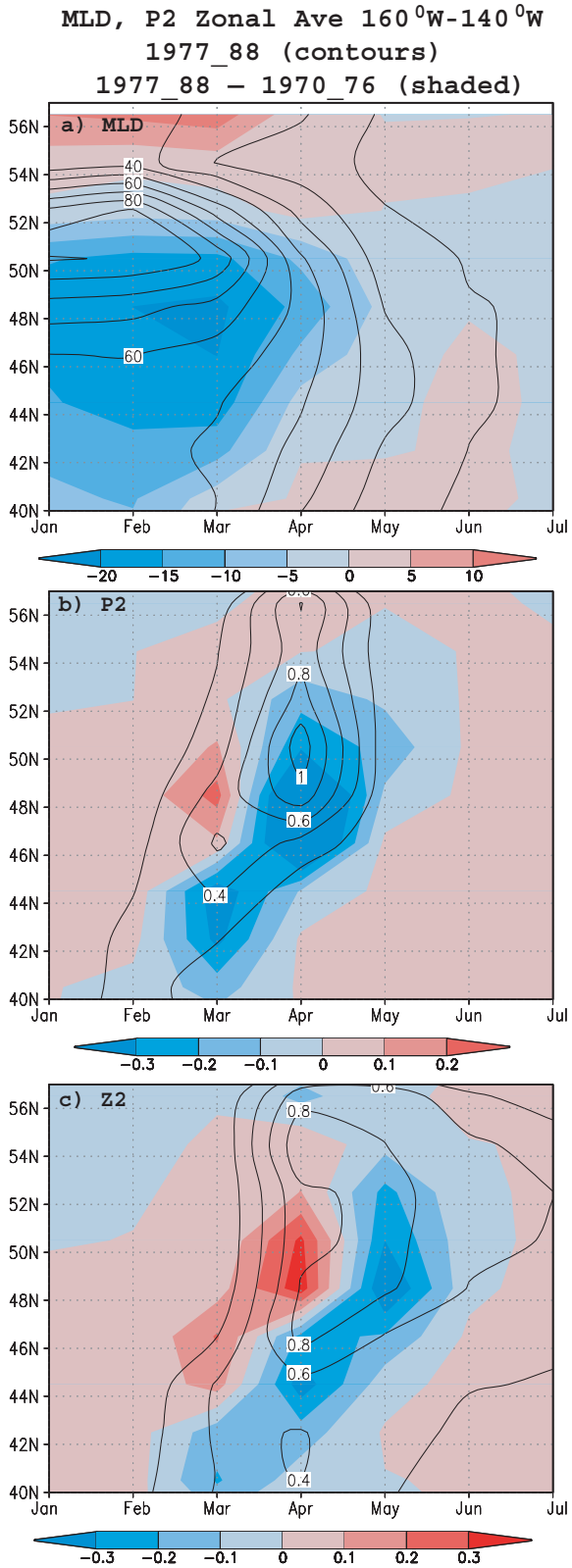

Fig. 7. Hovmöller (latitude-time) diagrams of the 1977-88 mean (contours) and Δ (shaded) values of a) MLD (m), b) P2 (mmol N m^{-3}) and c) Z2 (mmol N m^{-3}). The values are averaged over 160°W-140°W and shown for January through July.

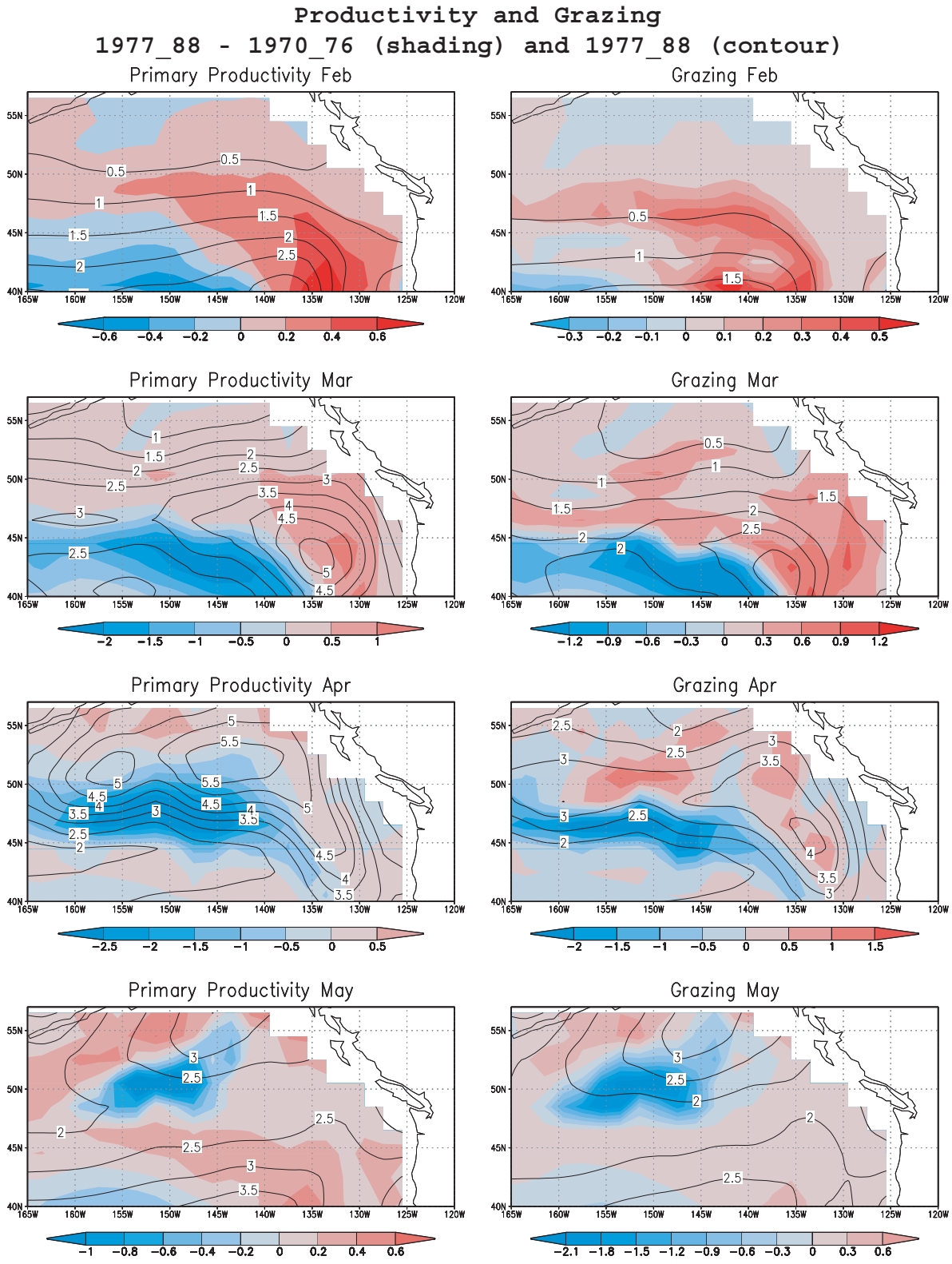

Fig. 8. The 1977-88 mean (contours) and Δ (shaded) P2 primary productivity (left column) and grazing of P2 by Z2 (right column) for the months of February, March, April, and May. The values have been averaged over the upper 150 m and are in units of mmol N m^{-2} day^{-1}.